

PSO for Graph-Based Segmentation of Wrist Bones in Bone Age Assessment

P. Thangam, K. Thanushkodi, T.V. Mahendiran

P. Thangam

Assistant Professor, CSE Department,
Coimbatore Institute of Engineering and Technology,
Coimbatore - 641109, Tamilnadu, India.
E-mail: saithangam@gmail.com

K. Thanushkodi

Director, Akshaya College of Engineering and Technology,
Coimbatore -642109, Tamilnadu, India.
Email: thanush12@gmail.com

T.V. Mahendiran

Assistant Professor, EEE Department,
Coimbatore Institute of Engineering and Technology,
Coimbatore - 641109, Tamilnadu, India.
E-mail: saimahegobi@gmail.com

Abstract:

Skeletal maturity is a reliable indicator of growth and skeletal bone age assessment (BAA) is used in the management and diagnosis of endocrine disorders. Bone age can be estimated from the left-hand wrist radiograph of the subject. The work presented in this paper proposes the development of an efficient technique for segmentation of hand-wrist radiographs and identifying the bones specially used as Regions of Interest (ROIs) for the bone age estimation process. The segmentation method is based on the concept of Particle Swarm Optimization (PSO) and it consists of graph-based segmentation procedure. The system provides an option of either segmenting all the bones totally or segmenting only the specific ROIs under consideration. The system is validated with a data set of 100 images with 50 radiographs of female subjects and 50 of male subjects. The time taken for segmenting each bone is calculated and the results are discussed.

Keywords: skeletal maturity, bone age assessment (BAA), particle swarm optimization (PSO), graph-based segmentation, left-hand wrist radiograph.

1 Introduction

The chronological situations of humans are described by certain indices such as height, dental age, and bone maturity. Of these, bone age measurement plays a significant role because of its reliability and practicability in diagnosing hereditary diseases and growth disorders. Bone age assessment using a hand radiograph is an important clinical tool in the area of pediatrics, especially in relation to endocrinological problems and growth disorders. A single reading of skeletal age informs the clinician of the relative maturity of a patient at a particular time in his or her life and integrated with other clinical finding, separates the normal from the relatively advanced or retarded. [1] The bone age of children is apparently influenced by gender, race, nutrition status, living environments and social resources, etc. Based on a radiological examination of skeletal development of the left-hand wrist, bone age is assessed and compared with the chronological age. A discrepancy between these two values indicates abnormalities in skeletal development. This is applied in the management and diagnosis of endocrine disorders.

2 Background of BAA

The main clinical methods for skeletal bone age estimation are the Greulich & Pyle (GP) method and the Tanner & Whitehouse (TW) method. GP is an atlas matching method while TW is a score assigning method. [2] GP method is faster and easier to use than the TW method. Bull et al performed a large scale comparison of the GP and TW method and concluded that TW method is the more reproducible of the two and potentially more accurate. [3] In GP method, a left-hand wrist radiograph is compared with a series of radiographs grouped in the atlas according to age and sex. The atlas pattern which superficially appears to resemble the clinical image is selected. TW method uses a detailed analysis of each individual bone, assigning it to one of eight classes reflecting its developmental stage (in terms of scores). The sum of all scores assesses the bone age. This method yields the most reliable results. In detail, in the TW method twenty regions of interest (ROIs) located in the main bones are considered for the bone age evaluation. Each ROI is divided into three parts: Epiphysis, Metaphysis and Diaphysis; it is possible to identify these different ossification centers in the phalanx proximity. The development of each ROI is divided into discrete stages, as shown in Figure 1, and each stage is given a letter (A,B,C,D, ...I), reflecting the development stage as:

- Stage A – absent
- Stage B – single deposit of calcium
- Stage C – center is distinct in appearance
- Stage D – maximum diameter is half or more the width of metaphysis
- Stage E – border of the epiphysis is concave
- Stage F – epiphysis is as wide as metaphysis
- Stage G – epiphysis caps the metaphysis
- Stage H – fusion of epiphysis and metaphysis has begun
- Stage I – epiphyseal fusion completed.

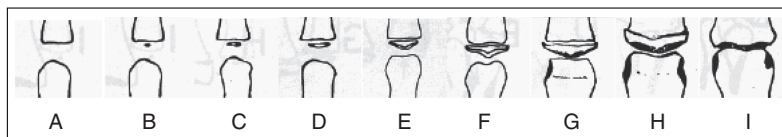


Figure 1: TW stages for phalanx bone.

By adding the scores of all ROIs, an overall maturity score is obtained. This score is correlated with the bone age differently for males and females. [4] Hence for accurate estimation of bone age, the ROIs are to be properly extracted and analyzed. So BAA requires efficient segmentation schemes for further processing. This paper proposes an efficient segmentation technique using graphs for segmenting the bones in the radiograph. We have done a thorough survey of literature on BAA methods in our previous work [5], explaining in detail the various work done in BAA and providing directions for future research. Our previous work [6] describes a computerized BAA method for carpal bones, by extracting features from the convex hull of each carpal bone, named as the convex hull approach. We have also proposed an automated BAA method to estimate bone age from the feature ratios extracted from carpal and radius bones, named as the feature ratio approach. [7] Our decision tree approach utilizes features from the radius and ulna bones and their epiphyses for BAA. [8] We have also exploited the epiphysis/ metaphysis region of interest (EMROI) in BAA using our Hausdorff distance approach. [9] A comparative study of

the above four BAA approaches has been conducted using partitioning technique. [10] We have also proposed an efficient method for feature analysis of radiographs using Principal Component Analysis (PCA) based on PSO. [11] The work presented in this paper is a novel method for segmenting the wrist bones from the input radiographs using PSO, applying the graph-based segmentation.

3 System Design

The system consists of three modules, namely: Image Preprocessing, Edge Detection and Graph-based segmentation.

3.1 Image Preprocessing

Image preprocessing is performed in two steps, image smoothing and grayscale conversion. Image smoothing is done to reduce the noise within the image or to produce a less pixelated image. Most smoothing methods are based on low pass filters. In our system, we have done smoothing to reduce noise by using a Gaussian filter. Gaussian filter reduces the magnitude of higher frequencies proportional to the lower frequencies, but at the cost of more computation time. But the speeding up of smoothing is achieved by splitting 2D Gaussian $G(x,y)$ into two 1D Gaussians $G(x)G(y)$ and carrying out filtering in 1D, first row by row and then column by column. Grayscale conversion is done as follows. Colors in an image are converted to a shade of gray by calculating the effective brightness or luminance of the color and using this to create a shade of gray that matches the desired brightness.

3.2 Edge Detection

Edge occurs where there is a discontinuity in the intensity function or a very steep intensity gradient in the image. Using this assumption, if one take the derivative of the intensity value across the image and find points where the derivative is maximum, then the edge could be located. [12] We have made use of Sobel edge detector to detect the edges. The Sobel operator performs a 2-D spatial gradient measurement on an image. Typically it is used to find the approximate absolute gradient magnitude at each point in an input grayscale image. The Sobel edge detector uses a pair of 3×3 convolution masks, one estimating the gradient in the x-direction (columns) and the other estimating the gradient in the y-direction (rows). A convolution mask is usually much smaller than the actual image. As a result, the mask is slid over the image, manipulating a square of pixels at a time. The actual Sobel masks [13] are given below:

-1	0	+1		+1	+2	+1
-2	0	+2		0	0	0
-1	0	+1		-1	-2	-1
G_x			G_y			

The magnitude of the gradient is then calculated using the formula:

$$|G| = \sqrt{G_x^2 + G_y^2} \quad (1)$$

An approximate magnitude can be calculated using:

$$|G| = |G_x| + |G_y| \quad (2)$$

3.3 Graph-based segmentation

Graph-based segmentation method [14] measures the evidence for a boundary between two regions by comparing two quantities:

- Intensity differences across the boundary and
- Intensity differences between neighboring pixels within each region.

Intuitively, the intensity differences across the boundary of two regions are perceptually important if they are large relative to the intensity differences inside at least one of the regions. Graph-based image segmentation techniques generally represent the problem in terms of a graph $G = (V, E)$ where each node $v_i \in V$ corresponds to a pixel in the image, and the edges in E connect certain pairs of neighboring pixels. A weight is associated with each edge based on some property of the pixels that it connects, such as their image intensities. Depending on the method, there may or may not be an edge connecting each pair of vertices. Let $G = (V, E)$ be an undirected graph with vertices $v_i \in V$, the set of elements to be segmented, and edges $(v_i, v_j) \in E$ corresponding to pairs of neighboring vertices. Each edge $(v_i, v_j) \in E$ has a corresponding weight $w((v_i, v_j))$, which is a non-negative measure of the dissimilarity between neighboring elements v_i and v_j .

The segmentation algorithm defines the boundaries between regions by comparing two quantities. The internal difference of a component C in an image is given by:

$$Int(C) = \max_{e \in MST(C,E)} w(e) \quad (3)$$

where $w(e)$ is the largest weight in the Minimum Spanning Tree (MST) of the component. The difference between two components C_1, C_2 which are vertices of the graph is defined to be the minimum weight edge connecting the two components, given by:

$$Dif(C_1, C_2) = \min_{v_i \in C_1, v_j \in C_2, (v_i, v_j) \in E} w((v_i, v_j)) \quad (4)$$

If there is no edge connecting C_1 and C_2 , we let $Dif(C_1, C_2) = \infty$. The region comparison predicate evaluates if there is evidence for a boundary between a pair or components by checking if the difference between the components, $Dif(C_1, C_2)$ is large relative to the internal difference within at least one of the components, $Int(C_1)$ and $Int(C_2)$.

3.4 Overview of PSO

Particle Swarm Optimization (PSO) is an algorithm for finding optimal regions of complex search space through interaction of individuals in a population of particles. PSO algorithm, originally introduced in terms of social and cognitive behavior by Eberhart and Kennedy in 1995 [15] has been proven to be a powerful competitor to other evolutionary algorithms such as genetic algorithms. PSO algorithm simulates social behavior among individuals (particles) flying through multidimensional search space, each particle representing a single intersection of all search dimensions. [16]–[19] The particles evaluate their positions relative to a global fitness at every iteration, and companion particles share memories of their best positions, and then use those memories to adjust their own velocities and positions. At each generation, the velocity of each particle is updated, being pulled in the direction of its own previous best solution (local) and the best of all positions (global). Computation of optimal threshold is handled here with Particle Swarm Optimization (PSO). Implementation of PSO algorithm analyzed here to find out the optimal threshold for segmentation. The population size of particles refers the number

of particles in iterative process, thus denoting components in the image here. A population of particles is initialized with random positions and velocities in d-dimensional space. A fitness function, f is evaluated, using the particle's positional coordinates as input values. Positions and velocities are adjusted, and the function is evaluated with the new coordinates at each time-step.

3.5 Implementation of PSO for graph-based segmentation

The implementation of the segmentation algorithm consists of the following steps.

Step 1: Swarm Formation: For a population size p , the particles are randomly generated between the minimum and the maximum limits of the threshold values.

Step 2: Objective Function evaluation: The objective functions of the particles are evaluated.

Step 3: 'pbest' and 'gbest' initialization: The objective values obtained above for the initial particles of the swarm are set as the initial pbest values of the particles. The best value among all the pbest values is identified as gbest.

Step 4: Velocity computation: The new velocity for each particle is computed using equation (5).

$$v[i] = v[i] + c_1 * rand(i) * (pbest[i] - present[i]) + c_2 * rand(i) * (gbest[i] - present[i]) \quad (5)$$

Step 5: Position computation: The new position for each particle is computed using equation (6).

$$present[i] = present[i] + v[i] \quad (6)$$

where, $v[i]$ is the particle velocity, $present[i]$ is the current particle (solution), $pbest[i]$ and $gbest[i]$ are defined as stated before, $rand(i)$ is a random number between (0,1), c_1 , c_2 are learning factors. Usually $c_1 = c_2 = 2$.

Step 5: Swarm Updation: The values of the objective function are calculated for the updated positions of the particles. If the new value is better than the previous $pbest$, the new value is set to $pbest$. Similarly, $gbest$ value is also updated as the best pbest.

Step 6: Termination: If the stopping criteria are met, the positions of particles represented by $gbest$ are the optimal threshold values. Otherwise, the procedure is repeated from step 4.

4 Results and Discussion

The use of image pre-processing techniques such as image smoothing and gray scale conversion improves the quality of the digitized radiograph. The noise caused due to radiation and other external factors are eliminated. Application of Sobel edge detector identifies the boundary of the bones or the regions of interest. This facilitates in better segmentation. Finally, the PSO algorithm for graph-based image segmentation is used to individually segment each bone in the left-hand wrist radiograph. The algorithm provides an option of whether to segment the entire radiograph (to identify all the bones in the radiograph) or to segment selected ROIs alone (some individual bone only). Figure 2 (a) depicts the input radiograph image, Figure 2 (b) denotes the image after smoothening, Figure 2 (c) provides a snapshot of edge detection using Sobel operator, Figure 2 (d) provides the snapshot of segmenting all the wrist bones in the left hand radiograph image, while Figure 2 (e) shows segmentation of selective ROIs (in this case the proximal, middle, and distal phalangeal bones). Figure 3 shows the graph depicting the performance assessment of the segmentation. The time taken to segment each bone using the PSO technique is calculated

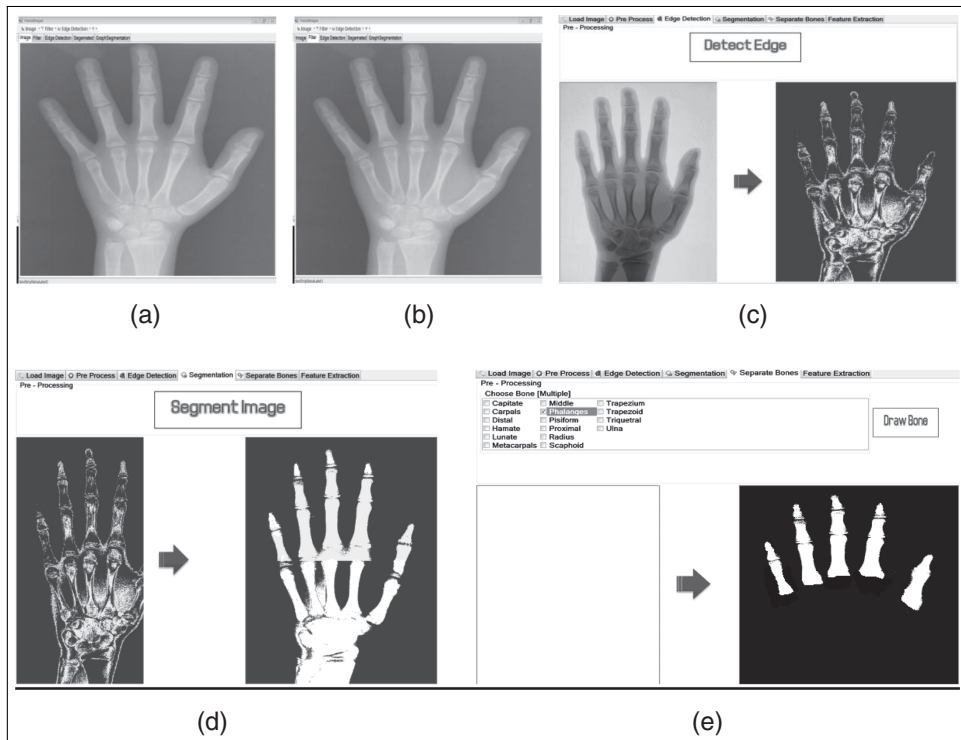


Figure 2: (a) Input radiograph image, (b) Smoothened image, (c) Edge detected image, (d) Segmenting all the bones in the image, (e) Segmenting selective (phalangeal) ROIs

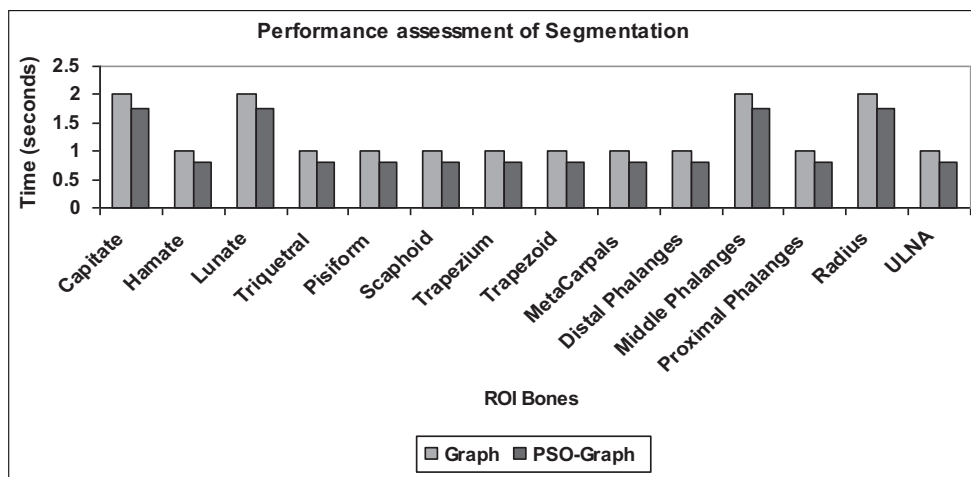


Figure 3: Performance Assessment of Segmentation

and is compared with the plain graph-based technique and the results are tabulated in Table 1. The segmentation was regarded as accurate if the sum of over selected and under selected pixels were less than 25. The segmentation process was accurate by 0.94 for males and 0.96 for females, as tabulated in Table 2. The PSO algorithm is implemented with the following parameters, *Population size*: 50, *max min w* = 0.6, *w* = 0.1, $C_1 = C_2 = 1.5$, *Iteration*: 50.

Table 1: Time taken for segmenting the ROI bones.

BONE NAME	Graph (sec)	PSO-Graph (sec)
Capitate	2	1.75
Hamate	1	0.8
Lunate	2	1.75
Triquetral	1	0.8
Pisiform	1	0.8
Scaphoid	1	0.8
Trapezium	1	0.8
Trapezoid	1	0.8
MetaCarpals	1	0.8
Distal Phalanges	1	0.8
Middle Phalanges	2	1.75
Proximal Phalanges	1	0.8
Radius	2	1.75
ULNA	1	0.8

Table 2: Experiment Results.

Sex	No. of Images	Accurate	Inaccurate	Accuracy
Male	50	47	3	0.94
Female	50	48	2	0.96

5 Conclusion

PSO algorithm was used for graph-based segmentation of left hand wrist radiograph images, which can be further used for skeletal bone age assessment. The input image was first pre-processed to remove noise and was grayscale converted to improve image quality. Sobel edge detector was used for edge detection and then PSO combined graph-based segmentation was performed. The segmentation procedure provided two options, whether to segment all the wrist bones as a whole or to segment selective ROI bones. The time taken to segment each bone was calculated and the results were tabulated. The system was tested with 100 left hand wrist images (50 males and 50 females). The quality of the segmentation was influenced by the image quality. For radiographs over exposed to radiation, further preprocessing was required, to achieve good results.

Bibliography

- [1] Gilsanz, V.; Ratib, O. (2005); *Hand Bone Age – A Digital Atlas of Skeletal Maturity*, Springer-Verlag.
- [2] Spampinato, C. (1995); *Skeletal Bone Age Assessment*, University of Catania, Viale Andrea Doria, 6 95125.
- [3] Bull, R.K.; Edwards, P.D.; Kemp, P.M.; Fry, S; Hughes, I.A. (1999); Bone Age Assessment: a large scale comparison of the Greulich and Pyle, and Tanner and Whitehouse (TW2) methods, *Arch. Dis. Child*, ISSN 1468-2044, 81: 172-173.

-
- [4] Tanner, J.M.; Whitehouse, R.H. (1975); *Assessment of Skeletal Maturity and Prediction of Adult Height (TW2 method)*, Academic Press.
- [5] Thangam, P.; Thanushkodi, K.; Mahendiran, T.V. (2011); Skeletal Bone Age Assessment – Research Directions, *International Journal of Advanced Research in Computer Science*, ISSN 0976-5697, 2(5): 415-423.
- [6] Thangam, P.; Thanushkodi, K.; Mahendiran, T.V. (2012); Computerized Convex Hull Method of Skeletal Bone Age Assessment from Carpal Bones, *European Journal of Scientific Research*, ISSN 1450-216X/1450-202X, 70(3): 334-344.
- [7] Thangam, P.; Thanushkodi, K.; Mahendiran, T.V. (2012); Efficient Skeletal Bone Age Estimation Method using Carpal and Radius Bone features, *Journal of Scientific and Industrial Research*, ISSN 0975-1084, 71(7): 474-479.
- [8] Thangam, P.; Thanushkodi, K. (2012); Computerized Skeletal Bone Age Assessment from Radius and Ulna bones, *International Journal of Systems, Applications and Algorithms*, ISSN 2277-2677, 2(5): 60-66.
- [9] Thangam, P.; Thanushkodi, K. (2012); Skeletal Bone Age Assessment from Epiphysis/Metaphysis of phalanges using Hausdorff distance, *Scientific Research and Essays*, ISSN 1992-2248, 7(28): 2495-2503.
- [10] Thangam, P.; Thanushkodi, K.; Mahendiran, T.V. (2012); Comparative Study of Skeletal Bone Age Assessment Approaches using Partitioning Technique, *International Journal of Computer Applications*, ISSN 0975 – 8887, 45(18): 15-20.
- [11] Thangam, P.; Thanushkodi, K.; Mahendiran, T.V. (2011); Efficient Feature Analysis of Radiographs in Bone Age Assessment, *International Journal of Computer Applications in Engineering Sciences*, ISSN 2231-4946, 1(2): 601-606.
- [12] Cooper, M.C. (1998); The tractability of segmentation and scene analysis, *International Journal of Computer Vision*, ISSN 0920-5691, 30(1): 27-42.
- [13] Gonzalez, R.C.; Woods, R.E. (2009); *Digital Image Processing*, Third Edition, Pearson.
- [14] Felzenswalb, P.F.; Huttenlocher, D.P. (2004); Efficient Graph-Based Image Segmentation, *International Journal of Computer Vision*, ISSN 0920-5691, 59(2): 167-81.
- [15] Kennedy, J.; Eberhart, R.C. (1995); Particle Swarm Optimization, *Proc of the IEEE International Conference on Neural Networks*, Australia, pp. 1942–1948.
- [16] <http://www.swarmintelligence.org/>
- [17] <http://www.particleswarm.info/>
- [18] Nedjah, N.; Mourelle, L.M. (2006); *Swarm Intelligent Systems*, Springer.
- [19] Kennedy, J.; Eberhart, R.C.; Shi, Y. (2001); *Swarm Intelligence*, Morgan Kaufmann Publishers.